Russian Geology and Geophysics © 2020, V.S. Sobolev IGM, Siberian Branch of the RAS
Vol. 61, No. 11, pp. 1298–1312, 2020 *DOI:10.15372/RGG2019164* *Geologiya i Geofizika*

Migrating Seismicity in the Lithosphere of the Baikal Rift Zone: Spatiotemporal and Energy Distribution of Earthquake Chains

A.A. Kakourova✉, **A.V. Klyuchevskii**

Institute of the Earth's Crust, Siberian Branch of the Russian Academy of Sciences, ul. Lermontova 128, Irkutsk, 664033, Russia

Received 19 February 2019; received in revised form 9 May 2019; accepted 10 October 2019

Abstract—Quasi-linear sequences of the epicenters of strong earthquakes, identified in many seismically active regions, are phenomenologically viewed as "migrations" of earthquake sources. Following this analogy, an earthquake chain is understood in this paper as a set of seismic events of different energies, leading to a quasi-linear one-way change in the position ("migration") of the successive epicenters of shocks on the surface of the lithosphere zone under study. Based on this statement, a formalized method for an azimuthal analysis of seismicity is developed, which allows one to identify and isolate earthquake chains from arrays of seismological data presented in the standard format of a catalog of earthquakes. As this method is tested on a catalog of earthquakes and a catalog of simulation events, all model chains of events and a large number of earthquake chains and simulation events are identified. It is indicated by isolating chains in a random field of simulation events that some of these earthquake chains can be formed by a random spatiotemporal combination of shocks. Migrating seismicity in the lithosphere of the Baikal rift zone (BRZ) is studied by applying the method of identification and isolation of earthquake chains to materials from the "Catalog of Earthquakes of the Baikal region". According to data on 52,700 earthquakes with a representative energy class $K_P \geq 8$, occurring in the Baikal region from 1964 to 2013, there are 2143 earthquake chains identified and isolated within an angular sector of azimuthal analysis $q = 10°$ (±5° from azimuth α to the epicenter). As the angular sector of azimuthal analysis increases to $q = 20°$ (±10°), there is an approximately twofold increase in the number of chains ($M = 4245$). As shown by the analysis and comparison of spatiotemporal distribution of earthquakes and earthquake chains, the spatiotemporal and energy distribution of chains of seismic events is formed by earthquake distribution in the BRZ. Beyond this zone, the chains are small in number. The established relationship between the distributions of earthquakes and earthquake chains in space, in time, and by energy indicates that in the epicentral field of seismicity of the BRZ, both "seismicity migration" chains and randomly formed chains ("pseudomigration" chains) are identified. The migrating seismicity of the BRZ is studied according to the seismicity statistics by using the criteria developed within the framework of the simulation base model of migrating seismicity to the results obtained. An index of seismicity migration activity (ISMA) that reflects a seismicity migration/pseudomigration ratio at the set level of significance is used to obtain distribution maps over the territory and graphs of changes over the years for this index. The maps show that small areas ISMA > 1 are seen in close proximity to rifting attractor structures (RASs), while seismicity migration in the rest of the BRZ is not statistically obvious. The graphs show that periods ISMA > 1 at three levels of significance are observed three to four years after the activation of RASs, which makes it possible to estimate the phase propagation velocity of a slow deformation perturbation of about 250–300 km/year. It is indicated by the results obtained that the migrating seismicity of the BRZ is directly related to the location and activations of RASs and that the RASs are the sources of local deformation perturbations in the BRZ lithosphere, which, among other things, manifest themselves in the implementation of seismicity migration chains.

Keywords: seismicity; Baikal rift zone; earthquake chains; seismicity migration; deformation perturbation; current geodynamics of the lithosphere

INTRODUCTION

Recently, attention to the problem of "migration" of earthquake sources has increased significantly: nearly ten articles have been published on this topic in *Geodynamics and Tectonophysics* only in 2018. This is probably due to the fact that the migration phenomenon makes it potentially possible to predict strong earthquakes by fairly simple seismicity monitoring methods because the spatial localization and dynamics of the migration process of earthquake sources fit well within the framework of an avalanche-unstable cracking (AUC) model with preparation and implementation of a strong earthquake (Myachkin et al., 1975). The phenomenon of migration of earthquake sources has become widely known due to the work of C.F. Richter (1958), which describes a change in the location of epicenters and the formation of a chain of strong earthquakes along the North Anatolian Fault in Turkey. Migration as a regular movement of sources of acoustic pulses has been recorded in rock samples (Sobolev, 1993). In a number of works, the migration of earthquake sources are considered as possible indicators of strong earthquakes (Bot, 1968; Mogi, 1968; Vil'kovich et al., 1974; Kasakhara, 1985; Ulomov, 1993).

✉Corresponding author.
E-mail address: anna2015@crust.irk.ru (A.A. Kakourova)

Based on modern concepts of the structure of the fault-block lithosphere and the spatiotemporal changes in the stress-strain state (SSS), the directed "displacements" of earthquake epicenters can be used to describe "seismicity migrations" (Levina and Ruzhich, 2015, p. 225), in a broad sense reflecting the phenomenon of spatiotemporal statistically significant direction of propagation of seismic events successive in time and space in the interblock media of the hierarchically ordered lithosphere. From the standpoint of tectonophysics and modern geodynamics, seismicity migrations as a geophysical phenomenon can be associated with single-sided translationally directed generation of earthquake sources in regions of seismotectonic destruction of the lithosphere, which, as assumed by (Vil'kovich et al., 1974; Vikulin, 2003; Bykov, 2005; Makarov and Peryshkin, 2016), is due to slow deformation wave fronts and packets passing along the fault systems. Seismotectonic destruction areas consist of aggregates of quasi-linear fault zones, so a change in the position of the shock epicenters on the lithosphere surface can reflect a translational quasi-linear change in the location of earthquake sources along the fault zones caused by migrations of the front and/or a packet of deformation effects in the depths of the lithosphere.

Theoretical and experimental studies (Guberman, 1979; Malamud and Nikolaevskii, 1983; Nevskii et al., 1991; Ulomov, 1993; Nikolaevskii, 1995; Psakh'e et al., 2001; Goldin, 2002) showed that the energy redistribution and activation of faults in block media are often due to the dynamics of slow deformation waves (Kuz'min, 2012; Makarov and Peryshkin, 2016; Bykov, 2018). This phenomenon is understood as perturbations of the SSS of the lithosphere, which are wave perturbations propagating from the perturbation source (boundaries of tectonic plates and faults) at velocities of 1–100 km/yr, which occupy an intermediate position between tectonic creep velocities and sound velocities in a geomedium. Direct measurements of the parameters of slow deformation waves are still few in number (Kuzmin, 2012) due to their low velocities and gradients: they are usually detected indirectly from variations in geophysical fields and seismicity provided that these variations are fairly pronounced in space and time. A large review of the state of the problem of slow deformation perturbations is given in (Sherman, 2013), and the current state of research on the nature of slow deformation waves is described in (Makarov et al., 2018). It is shown in these papers that, despite more than half a century of history, the problems of spatiotemporal migration of geodynamic processes and slow deformation waves, which are considered to be the cause of migration in the lithosphere, remain some of the most controversial in tectonophysics, modern geodynamics, and geomechanics. At present, the efforts of many researchers are mainly aimed at identifying the slow perturbations of geodynamic fields, which are quasi-periodic and can be interpreted as slow deformation waves. These studies are carried out both in Russia and abroad and are based on the study of predominantly strong earthquakes. "Fast" deformations play a much smaller role due to their implicit relation with strong earthquakes and the lack of modern methods of statistical analysis of the spatiotemporal migrations of weak shocks.

Seismicity migrations as a reflection of the migration of current geodynamic processes in the spatiotemporal distribution of earthquakes were identified in many seismically active regions of the Earth (Richter, 1958; Mogi, 1968; Kasahara, 1985; Ulomov, 1993; Vikulin, 2003), including the BRZ lithosphere. It was revealed that those processes were controlled by active faults (Sherman and Gorbunova, 2008), and their cause could be deformation waves. It was possible to use the analysis of the spatiotemporal distribution of strong earthquakes in the zones of dynamic influence of faults to identify the general directions of migration activation of the main fault segments of the BRZ: from west to east in the southwestern and central parts of the zone and from east to west in the northeastern part of the territory, with the change of direction occurring approximately along a longitude of 109°. The study of seismicity migrations by the method of constructing spatiotemporal diagrams was carried out in (Levina and Ruzhich, 2015). The spatiotemporal analysis of the total seismic energy made it possible to identify three clusters of seismicity migrations developing along the BRZ from the southwest to the northeast and in the opposite direction. It was assumed that that deformation waves could be the cause of seismicity migration, and the seismicity migration process should be considered as a manifestation of a whole spectrum of deformation waves with different velocities. In (Novopashina, 2013), a method of spatiotemporal sweep of $\lg E_{sum}$ (the logarithm of the total seismic energy) with a spectral-temporal analysis in the "direction – time – $\lg E''_{sum}$ coordinate system (2013) was applied. Slow migrations of that parameter were revealed with velocities from kilometers to the first tens of kilometers per year, directed from the northeast to the southwest of the BRZ and back. A significant drawback of those methods was the lack of formalization in the determination and selection of the "migrating" parameter and predominantly an expert approach, while the use of total seismic energy did not allow one to identify and describe "migrations" as a regular spatiotemporal sequence – an earthquake chain (the number of shocks in a chain, the azimuth, the rate of change in the position of the epicenters). The methods were implemented for strong and moderate earthquakes, although they were applied in some cases for sequences of shocks of different energies. It should be noted that the phenomena of migration of earthquake sources identified in the BRZ were a priori considered to be seismicity migrations unambiguously caused by seismotectonic and geodynamic processes in the lithosphere.

The existing ideas about the migration of sources of strong earthquakes as a translational change in the position of shock hypocenters along the fault surface can be transferred to weak earthquakes. This can make it possible to study the phenomenon of earthquake sources migrations statistically and in more detail using a large amount of factual

data. In contrast to the migration of sources of a small number of strong earthquakes, among which the migration parameter is selected by an expert using spatiotemporal diagrams, one establishes the migration of sources in a large array of weak shocks by developing a formalized method for identifying and isolating earthquake chains. In this study, a formalized method for identifying and isolating earthquake chains is used (Klyuchevskii et al., 2018), which is based on the azimuthal analysis of a large number of shocks of various energy classes, presented in the standard format of a catalog of earthquakes. This method helps us obtain a large database of earthquake chains of the BRZ (Kakourova and Klyuchevskii, 2018), which makes it possible to perform a statistical analysis of the spatiotemporal and energy distribution of chains, reveal patterns and features of distributions in order to describe migrating seismicity in application to the models of modern geodynamics of the BRZ lithosphere.

METHOD AND MATERIALS

Materials for this study are taken from the "Catalog of Earthquakes of the Baikal Region" made by a free processing group of the Baikal Department of the Unified Geophysical Survey of the Russian Academy of Sciences (BD FBIS FRC UGS RAS) (http://www.seis-bykl.ru/). The study contains data on 52,700 earthquakes of representative energy classes $K_P \geq 8$, recorded on the territory of the Baikal region (φ = 48.0–60.0° N, λ = 96.0°–122.0° E) between 1964 and 2013. The map showing epicenters and the density isolines of earthquake epicenters in 0.2°×0.3° areas (Fig. 1) that seismic events are concentrated in the form of bands of predominantly northeast-southwest orientation according to the location and orientation of the zones of the main seismically active faults. Local high-density groups of shock epicenters often result from aftershock and swarm activity. Adjacent territories significantly differ in seismicity: the map clearly shows the contour of the highly seismic BRZ bounded by the virtually aseismic Siberian platform and the weakly seismic Transbaikalia. On the southwestern flank of the BRZ (area 1, φ = 48.0°–54.0° N, λ = 96.0°–104.0° E), shock epicenters are scattered over the territory, which is confirmed by an increased fractal box-counting dimension $D_0 \approx 1.60$ (Klyuchevskii and Zuev, 2007). This "areal" geometry of the shock distribution is due to the seismotectonic activation of sublatitudinal and sublongitudinal faults (Logachev, 2003). The epicentral field of the central part (area 2, φ =

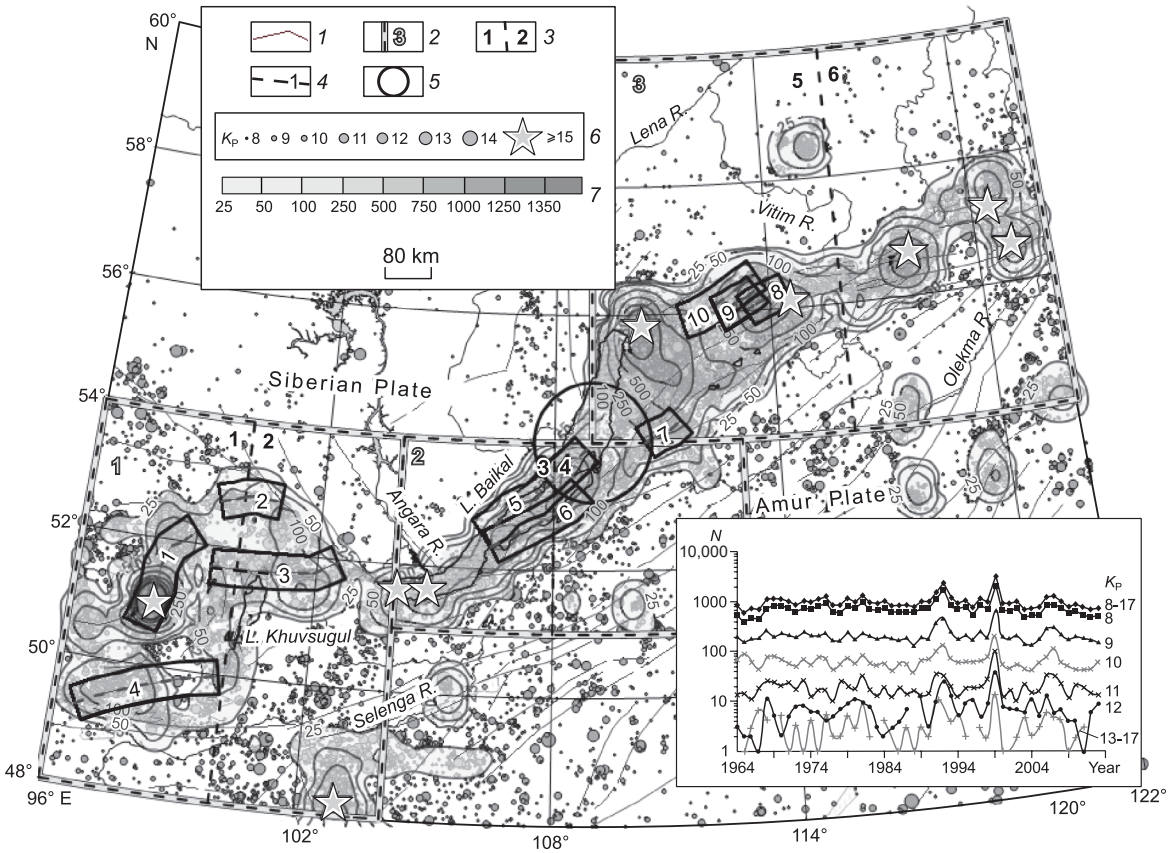

Fig. 1. Map of the epicenters and epicenter density isolines of 52,700 earthquakes of the Baikal Rift Zone with $K_P \geq 8$ (1964–2013). The inset shows the charts of annual numbers N of earthquakes of the BRZ with $K_P \geq 8$ and the samples of shocks of individual energy classes. *1*, main faults, *2*, boundaries and numbers of areas, *3*, boundaries and numbers of sections, *4*, boundaries and the numbers of the main seismically active fault zones (Tunka Fault No. 3), *5*, round area of a raidus R = 100 km (the center of the circle has coordinates φ = 54.0° N, λ = 109.0° E), *6*, earthquake epicenters of representative energy classes, *7*, scale of epicenter density in the 0.2×0.3° areas.

51.0°–54.0° N, λ = 104.0°–113.0° E) and the northeastern flank of the BRZ (area 3, φ = 54.0°–60.0° N, λ = 109.0°–122.0° E) has the form of a band located southeast and south of the Siberian Platform in the contact zone of the powerful craton and the Amur (North China) Plate. The box-counting dimension of the seismicity of these territories does not reach $D_0 < 1.5$ (Klyuchevskii and Zuev, 2007), which indicates band compression of the epicenter field. This "band" geometry of the shock distribution is caused by the activation of riftogenic faults of the northeastern (area 2) and sublatitudinal (area 3) strikes (Golenetsky, 1990; Misharina and Solonenko, 1990). In order to investigate seismicity in detail, the three areas are usually divided in half along the longitude λ = 100.0°, λ = 108.0°, and λ = 116.0° into six sections whose numbering starts from the southwest. Earthquake epicenter distribution over these areas is characterized by a decrease in the box-counting dimension from the first ($D_0 \approx 1.60$) to the sixth ($D_0 \approx 1.37$) area (Klyuchevskii and Zuev, 2007), i.e., the transformation of the epicenter field from the southwest to the northeast of the BRZ from a scattered "areal" geometry to a compressed "band" rift structure. The inset (Fig. 1*a*) shows the graphs of annual numbers N of earthquakes of the BRZ with $K_P \geq 8$ and samples of shocks of individual classes. Against the general average background in 1992 and 1999, the maxima of N are distinguished, which are caused by the aftershocks of the Busiyngol (December 27, 1991; $K_P = 16.2$; φ = 50.98° N, λ = 98.08° E), South-Baikal (February 25, 1999; $K_P = 14.6$; φ = 51.64° N, λ = 104.82° E), and Kichera (March 21, 1999; $K_P = 14.5$; φ = 55.83° N, λ = 110.34° E) earthquakes.

The term "earthquake chain" was originally used in (Lukk, 1978) to characterize the linear structure of epicenters related in space and time by sequences of weak shocks that contributed to the "rapid" deformation of the Earth's crust material. An earthquake chain was assumed to be a "linear sequence of randomly distributed epicenters of five or weaker earthquakes (K = 6–10) with a frequency of at least one day between successive events in time and 25 km in distance between neighboring epicentres" (Lukk, 1978, p. 27). If possible, random spatiotemporal sequences of earthquakes were excluded from consideration by setting a minimum number of events in a chain to be sufficiently large: five shock epicenters. Events differing from each other by no more than five catalog numbers were considered to be "successive", which reduced the probability of a nonrandom chain formation. It was found that the predominant range of energy classes of earthquakes in the chains was K = 6–8, while earthquake chains in general reached 10% of the total number of earthquakes. Earthquake chains were observed within a limited number of relatively narrow linear zones, which in some cases correspond to known disruptions in the Earth's crust (faults). It was assumed that temporal variations in chain density could be used to predict earthquakes.

In the "Catalog of Earthquakes in the Baikal Region", seismic events are characterized by five main parameters: hypocenter coordinates (latitude φ, longitude λ, and depth h), time in the focus t_0, and energy class K_P. It should be noted that the depths of hypocenters h of the earthquakes occurring in the BRZ are determined rarely and with low accuracy. For this reason, the "Catalog of Earthquakes of the Baikal Region" has been analyzed for more than half a century by four parameters: φ, λ, t_0, and K_P. These parameters are used to determine earthquake chains, and the simplest option is to analyze the earthquakes of a single energy class, but the analysis of a sample of earthquakes in the full range of classes does not change the technical essence of the method used. In general, an earthquake migration chain is understood as a phenomenon of a quasi-linear one-sided change in the location of successive epicenters of shocks on the lithosphere surface, which occurs under the influence of some geophysical and/or geodynamic processes, such as fluid migration, changes in the SSS, etc. Based on this formulation and the parameters available in the catalog, a method for identifying earthquake chains has been developed (Klyuchevskii et al., 2018). According to the formula of the method, the materials from the "Catalog of Earthquakes of the Baikal Region" are used to construct a map showing the earthquake epicenters of the territory under study and a schematic map of the azimuth vectors of the epicenters of successive shocks is developed. According to this schematic map of azimuth vectors, number n of successive (one after another) earthquakes directed in azimuth α is identified in a given angular sector of azimuthal analysis q°. If $n \geq 3$, then this shock sequence is defined as an earthquake chain in the epicentral seismicity field of a given territory and entered into the catalog of chains. Chains are cataloged sets of $n \geq 3$ successive (one after another) earthquakes provided that the shocks are in a given angular sector of permissible nonlinearity ± q/2° relative to azimuth α.

It is noteworthy that, if shocks in an earthquake chain occur at the same depth, then shock epicenters are displaced relative to the fault line on the lithosphere surface by the same amount at any angle of incidence of the fault, i.e., they represent a quasi-linear sequence of events – a chain. If shock hypocenters in an earthquake chain are located at different depths, then epicenter displacements relative to the fault line have different values depending on the angle of incidence of the fault. So, if the difference in the depths of the shock hypocentres is 20 km and the angle of incidence of the fault is 45°, their relative deviation from linearity is 20 km too. If the distance between these shocks is 100 km, they form an earthquake chain at $q \approx 20$°; if the distance is 200 km, then $q \approx 10$°. The greater the angle of incidence of the fault, the smaller the relative deviation of the epicenters from linearity, with the deviation being minimal at an angle of about 90°. It is known that the angles of incidence of seismically active faults in the BRZ have a distribution peak in a range of 50–60° with an average value of 53 ± 18° (Klyuchevskii, 2014a; Dem'yanovich and Klyuchevskii, 2018a). The overwhelming majority of the BRZ faults are longer than 150 km (Dem'yanovich et al., 2007), which means that the angular sector value optimal for identifying

and isolating earthquake chains at different depths is as follows: q = 10–20°.

The method is tested by additionally introducing data on model linear chains of events simulating set migrations of earthquake sources. The chains are identified and isolated under identical conditions in the epicentral fields of earthquakes and in the fields of randomly distributed simulation events. For this purpose, "Catalogs of Simulation Events" are developed within the same format as "Catalog of Earthquakes of the Baikal Region", and the "epicenters" of simulation events are generated within the framework of round and rectangular areas. In this case, the basis comprises two model representations of the epicentral field, briefly described above and reflecting the main properties of spatiotemporal distribution of seismicity of the BRZ. In the first model, on a round area, the simulation events have "areal" location, an "epicenter" field scattered over the surface, which means that these events are distributed randomly at a constant probability density. This model in the first approximation reflects the "areal" location of the earthquake epicenters, which is due to a set of several zones of seismically activate faults of different orientation as in the southwestern flank of the BRZ. In the second model, on a rectangular area, the simulation events are localized at the central part of the area near a virtual "fault" line, which means that these events are distributed randomly at a constant probability density along the area and according to the normal law across the area. This "band" distribution of the earthquake epicenters is observed at the central part and in the northwestern flank of the BRZ, as well as in most fault zones. This model in the first approximation reflects the structural zoning of faults (Lobatskaya, 1987) and the structure of the epicentral field of the seismically active fault zone (Dem'yanovich and Klyuchevskii, 2018b). Randomly distributed coordinates of the "epicenters" of simulation events are generated using a random number generator. Normal distribution of events is simulated using the Box–Muller transform (Box and Muller, 1958) for coordinate y of generated points, which converts a randomly distributed value and a normal distribution.

RESULTS

Test and model examples. *Earthquake chains and simulation event chains in a round area.* In a test example, earthquake chains in several fault zones are identified and isolated for an epicenter field of 950 shocks with an energy class K_P = 8 (Fig. 1*a*, Supp.[1]), which have occurred on a small territory at the central part of the BRZ between 1980 and 2004. A schematic map of the epicenter earthquakes of this territory is shown as a circle of a radius R = 100 km, and the circle center coordinates are φ = 54.0°N, and λ = 109.0° E (Fig. 1). In azimuths, α_1 = 25°, α_2 = 75°, and α_3 = 225°, the epicentral field of earthquakes is supplemented with the "epicenters" of model linear chains comprised of n_1 = 3, n_2 = 4, and n_3 = 5 successive events whose parameters are inserted into the central part of the original array of 950 shocks and separated from each other by data on earthquakes. Epicenter density isolines are drawn through the values of the shock numbers in round areas of radius r = 10 km, and smoothing is carried out by overlapping the areas by r = 10 km in latitude and longitude. Earthquake epicenters are recorded as bands, reflecting the fact of implementation of faults of northeastern–southwestern orientation in subparallel zones (Fig. 1*a*, Supp.). The temporal analysis of the schematic map of azimuth vectors of earthquake epicenters in an angular sector of a size q = 10° (Δq = ±5° from azimuthal direction) helps us determine and allocate three chains comprised of n_1 = 3, n_2 = 4, and n_3 = 5 events (Fig. 1*b*, Supp.), whose location and orientation fully matches the inserted model chains of events. Among 950 earthquakes, 22 chains are identified and isolated (Fig. 1*b*, Supp.; vectors from the epicenter of the first earthquake to that of the last one): the vectors characterize the position, length, and azimuth of the chain orientation. There is a systemic distribution of chains by location and orientation azimuth, associated with fault zones: the location corresponds to zones of higher density of earthquake epicenters, and almost all chains have northeastern-southwestern linearity corresponding to the fault orientation and the elongation of the epicenter density isolines (see in Fig. 1*a*, Supp.).

As a test model example, we present the results of identifying and isolating chains in the field of "epicenters" of 950 simulation events distributed randomly with a constant probability density on the surface of a round area with a radius of R=100 km (Fig. 2*a*, Supp.). Model linear chains comprised of n_1 = 3, n_2 = 4, and n_3 = 5 events are inserted, and event density isolines are drawn in the same way as for earthquakes from a real area. Simulation events are distributed fairly evenly, and there are no significant density extremes (Fig. 2*a*, Supp.), which is associated with event generation conditions. Following the temporal analysis of the schematic map of the azimuth vectors for an angular sector of q = 10°, three chains of n_1 = 3, n_2 = 4, and n_3 = 5 events are identified and isolated (Fig. 2*b*, Supp.), and their location matches the model chains of events. Among 950 simulated events, 15 chains with nonsystemic distribution by location and orientation azimuth are identified and isolated. It is noteworthy that isolating chains in a random field of simulation events corresponds to the results obtained previously (Klyuchevskii and Kakourova, 2016, 2018a) and indicates that some of the earthquake chains can be formed and isolated with a random spatiotemporal combination of shocks.

Earthquake chains and simulation events in a rectangular area. An epicentral field of 1224 earthquakes with $K_P \geq 8$, which occurred in the Tunka Fault Zone (see Fig. 1, the fault number 3 in the central part of the southwestern flank of the BRZ) from 1964 to 2014, is presented on a schematic map of the disjunctive zone, whose length is

[1] Supplement materials http://sibran.ru/journals/Suppl.pdf.

equal to that of the fault (L~226 km) (Fig. 3*a*, Supp.). Three western sublatitudinal segments of the fault, which slightly differ in orientation in geographic coordinates in Fig. 1, in linear coordinates L and W are combined into one rectangle of a width W = 60 km wide (±30 km from the fault line on the surface), and a fourth eastern segment of the fault at an angle and with northeast orientation is added to them. Epicenter density isolines are drawn according to the number of shocks in square areas with a side of 10 km, and smoothing is carried out by overlapping the areas by 5 km in latitude and longitude. Earthquakes are distributed along the fault zone with an average density of 10–15 epicenters per 100 km^2 (Fig. 3*a*, Supp.). The density of earthquake epicenters is significantly increased on both sides of the break of the fault at a distance $L \approx$ 135–160 and $L \approx$ 175–200 km, with the density maxima reaching 90 shocks. The earthquake distribution across the fault zone is generally normal, with a maximum density near the fault line. Model linear chains of $n_1 = 5$, $n_2 = 4$, and $n_3 = 3$ events are inserted into this earthquake epicenter field at distances of 5, 15, and 25 km from the fault line, respectively, thereby simulating migrations in the fault zone. The data on model chains are included in the central part of the array of 1224 shocks, and the chains in the catalog are separated from each other by earthquakes. Following the temporal analysis of the schematic map of the azimuth vectors with an angular sector q = 10°, three chains of $n_1 = 5$, $n_2 = 4$, and $n_3 = 3$ events are identified and isolated (Fig. 3*b*, Supp.), whose location corresponds to the inserted model chain of events. Among 1224 earthquakes, 66 chains are identified and isolated (shown in Fig. 3*b*, Supp., in the form of vectors). The systemic character of the chain distribution by location and azimuth of orientation is clear: the location corresponds to zones of increased density of earthquake epicenters, almost all chains are concentrated near the fault and have an orientation corresponding to the orientation of the Tunka fault and the elongation of the epicenter density isolines (Fig. 3*a*, Supp.).

As a test model example, we present the results of identifying and isolating chains in the "epicentre" field of 1224 simulation events distributed along a rectangular area of a length L = 226 km and a width W = 60 km (±30 km from the virtual "fault" line) randomly with a constant probability density (Fig. 4*a*, Supp.). Across the area, the event "epicenters" are distributed according to the normal law. Model linear chains of $n_1 = 5$, $n_2 = 4$, and $n_3 = 3$ events are inserted, and the event density isolines are drawn the same way as for earthquakes (see Fig. 3*a*, Supp.). The simulation events are accumulated near the "fault" line, and there are no significant density extrema along the area. Following the temporal analysis of the schematic map of the azimuth vectors at an angular sector q = 10°, three chains of $n_1 = 5$, $n_2 = 4$, and $n_3 = 3$ events are identified and isolated (Fig. 4*b*, Supp.), whose location corresponds to the inserted model linear chains. Among 1224 events, 85 chains are identified and isolated (shown in Fig. 4*b* with additional materials as vectors). Chain distribution by located and azimuth of orientation is set by the "fault" zone: almost all chains are accumulated near the "fault" line, and their orientation corresponds to that of the "fault" and elongation of the "epicenter" density isolines (see Fig. 4*a*, Supp.). Isolating the chains in a random field of simulation events of the rectangular area corresponds to the results obtained previously (Kakourova and Klyuchevskii, 2017) and the conclusion that some earthquake chains in the rectangular fault line can be identified and isolated in a random spatiotemporal distribution of shocks.

Spatiotemporal and energy distribution of earthquake chains in the BRZ lithosphere. The testing of this method confirms that it can be practically applied to determine and allocate earthquake chains in the epicentral seismicity field. In order to obtain the concept of spatiotemporal and energy distribution of earthquake chains in the BRZ lithosphere, we apply this method to 52,700 earthquakes given in Fig. 1. The calculations and operations carried out in the epicentral seismicity field of the BRZ at q = 10° (±5° from azimuth α) result in identifying and isolating 2143 earthquake chains whose location and orientation are shown as vectors on the schematic map (Fig. 2). Among the isolated chains, sequences of three earthquakes (M_3 = 2098) are predominant, which are significantly smaller than the chains of four shocks (M_4 = 45). In general, the earthquake chains are about 13% of the general number of earthquakes, which is slightly larger than in the Garm Region of Tajikistan (Lukk, 1978). It should be noted that, as the angular sector of azimuthal analysis increases up to q = 20° (±10° from α), there is an approximately twofold increase in the number of identified and isolated chains up to 4245 (M_3 = 4105, M_4 = 135, and M_5 = 5). A similar tendency is observed in identifying and isolating earthquake chains among the seismic events of individual energy classes. The only exception is strong earthquakes with $K_P \geq 13$, with their number of chains slightly increasing as the sector size increases. The locations of the epicenters of the first shocks of chains (the beginning of a chain) are used to calculate the epicenter densities in 0.2°×0.3° areas and draw the density isolines of the beginning of the chains. Figure 2 clearly shows that the vector azimuths correspond well to the location and northeastern-southwestern orientation of the zones of the main seismically active faults of the BRZ in Fig. 1, and the chain density maxima usually correspond to the zones of high density of shock epicenters.

The inset (Fig. 2) shows the charts of annual numbers of earthquake chains M, identified and isolated at q = 10° from a sample of shocks with $K_P \geq 8$ and from a sample of shocks of individual classes (K_P = 8, K_P = 9,… K_P = 12, $K_P \geq 13$). It can be seen that the maximum number of chains is formed by weak shocks with K_P = 8–9, and the number of chains decreases as K_P becomes larger. The main maxima M are isolated in 1992 and 1999 and correspond to the maximum of the numbers of earthquakes N in Fig. 1. There are time intervals with a small number of isolated earthquake chains, which indicates the changing dynamics of the formation of earthquake chains in the BRZ lithosphere. The paired linear

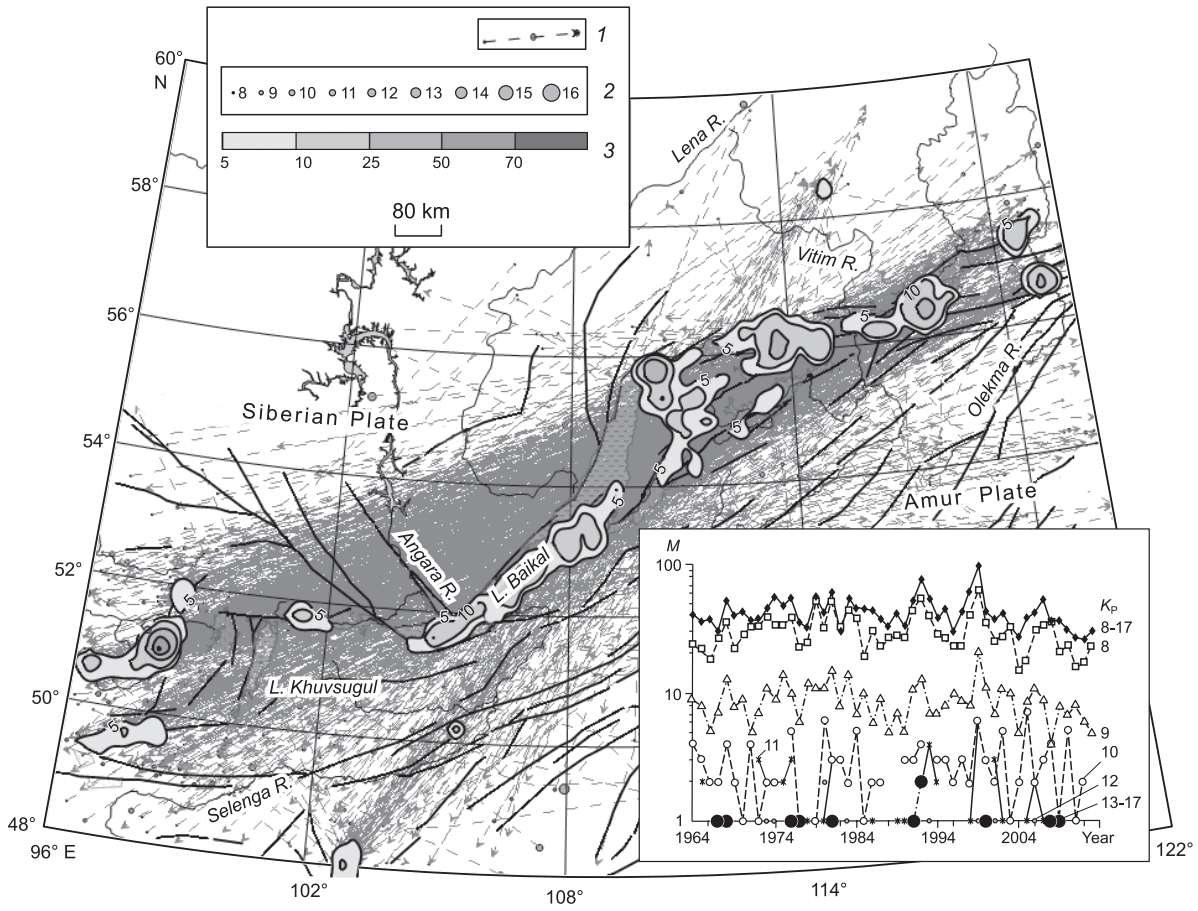

Fig. 2. Schematic map of the location and orientation of 2143 earthquake chains in the BRZ lithosphere, identified and isolated at q = 10°. The inset shows the charts of the annual numbers of earthquake chains M, identified and isolated from a sample of shocks with $K_P \geq 8$ and from the samples of shocks of individual classes ($K_P = 8$, $K_P = 9$,… $K_P = 12$, $K_P \geq 13$). *1*, earthquake chain vectors, *2*, epicenters of the first earthquakes in a chain, *3*, a scale of epicenter density isolines of the first earthquakes in chains. For the rest of the legend, see Fig.1.

correlation coefficients of the annual numbers of earthquakes N (Fig. 1) and the annual numbers of chains M have high values ($\rho > 0.65$) for the samples of shocks with $K_P \geq 8$, $K_P = 8$, and $K_P = 9$, but, for earthquakes with $K_P \geq 10$, the correlation coefficient drops sharply ($\rho < 0.35$). In the distribution of the number of earthquake chains with $K_P \geq 11$, four groups can be distinguished with no chains between them, and chains with $K_P = 11$ and $K_P = 12$ usually precede chains of strong earthquakes with $K_P \geq 13$ (magnitude $M_{LH} \geq 5$).

In order to analyze the earthquake chain density distribution, the BRZ territory is divided into square areas 100 × 100 km^2 in size with an overlap of half the area in latitude and longitude. In the areas, the earthquake chains are isolated in a sector q = 10°, and a schematic map for the chain density isolines is constructed (Fig. 3). The map shows that, within the framework of the BRZ, a united zone of high density of chains ($M \geq 5$) is formed. In some areas, more than 100 chains are isolated, more than 120 chains are observed in the aftershock region of the earthquake in the vicinity of aftershocks of the Kichera River earthquake from 1999, while no earthquake chains are observed beyond the BRZ. It should be noted that the schematic map of the earthquake chain density is in good correspondence with the shock epicenter density map shown in Fig. 1. It is shown by analyzing the chain number distributions M by the energy classes of earthquakes K_P that the main mass of BRZ chains is formed by weak shocks with $K_P = 8$ and $K_P = 9$ (Table 1; Fig. 3). The ratio of the numbers of one class, identified and isolated in the angular sectors of azimuthal analysis q = 20° and q = 10°, is approximately equal to two. With q = 10° and q = 20°, the equations of pair linear correlation of the logarithm of the number of chains and the energy class of earthquakes are written as $\lg M = -0.44K_P + 6.63$ and $\lg M = -0.47K_P + 7.19$, respectively, at high correlation coefficients ≈0.99. Considering the fact that the samples of the chains of strong earthquakes combine all shocks with $K_P \geq 13$, the linear approximation of relationship $\lg M = f(K_P)$ has slopes close to the slope of the chart showing the recurrence frequency of earthquakes of the BRZ $\gamma \approx -0.50$ (Klyuchevskii, 2007).

Figure 4*a* shows the distribution histograms of the numbers of chains M with respect to azimuth α. It can be seen that these distributions have a normal form with maxima at azimuths of 50–60° and 240–260° for a complete sample of data and for individual classes, while the numbers of chains

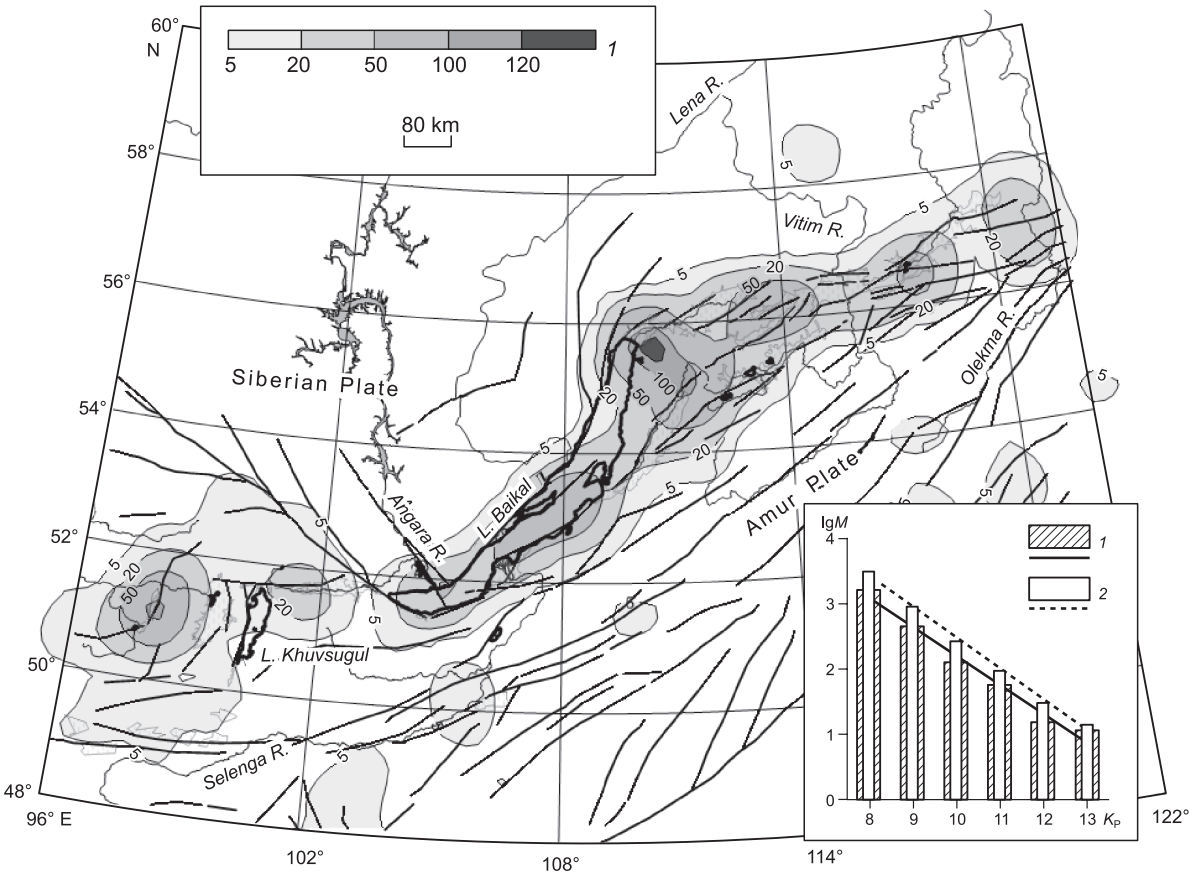

Fig. 3. Schematic map of the density isolines of the BRZ earthquake chains, identified and isolated at $q = 10°$ in the 100×100 км^2 areas. Inset shows the distributions of the logarithm of the numbers of chains M by K_P, identified and isolated at $q = 10°$ (1) and $q = 20°$ (2), and the correlation charts, respectively. *1*, scale of the density isolines of earthquake chains. For the rest of the legend, see Fig.1.

with azimuths of the eastern and western components almost match (1053 and 1090). Figure 4*b* shows a rose diagram of the distribution of the numbers of chains of moderate and strong earthquakes with $K_P = 11$, $K_P = 12$, and $K_P \geq 13$ with respect to α. It can be seen that the azimuths of the chains of strong earthquakes of the BRZ are consistent with the distributions in Fig. 4*a*.

Seismicity migrations in the BRZ lithosphere. A formalized technique for identifying and isolating earthquake chains allows one to obtain a large amount of factual material for a statistical study of spatiotemporal and energy patterns and the manifestation of earthquake chains in seismically active regions and zones, whose size and shape are set by an operator on the basis of the task at hand and the structure of the shock distribution. However, as noted above, some of the identified and isolated earthquake chains are not migrations of earthquake sources (seismicity migrations), but are created by a random spatiotemporal combination of shocks ("pseudomigration"). This is proven by the proportionality of ratios between the number of earthquakes and the number of chains in their spatiotemporal and energy distributions (see Fig. 1/Fig. 2 and Fig. 1/Fig. 3), as well as the isolation of chains among simulation events with a random distribution. The spatiotemporal and energy distributions of the numbers of earthquake chains shown in Figs. 2 and 3 indicate a relationship between the numbers of the isolated chains M and the spatiotemporal distribution density of the shocks that have occurred N – the higher the shock density and the velocity of the seismic flow, the more earthquake chains are isolated. Elementary estimates show that, in a fault zone with two possible directions of migration, the probability of isolating a chain of three successive random shocks is quite high ($P = 1/2 \cdot 1/2 = 1/4$). Therefore, the study of migratory seismicity of the BRZ, based on the seismicity statistics of the Baikal region, areas, sections, and active fault zones, which contains a random spatiotemporal set of earthquakes and a deterministic component of migrating seismicity, requires that the criteria by which the level of seismicity migration can be estimated at a background of randomly distributed earthquakes are applied to the results obtained. This problem is solved in this work by using the results obtained earlier within the framework of a simulation basic migrating seismicity model (Klyuchevskii and Kakourova, 2016, 2018a; Kakourova and Klyuchevskii, 2017). In these works, numerical methods are used to determine criteria for identifying earthquake chains in epicentral fields of

Table 1. *ISMA* for the earthquake chains of the BRZ in different ranges of energy classes K_P with account for one, two, and three standard deviations σ

K_P	N	M	$\overline{M}$	σ	ISMA	$ISMA_\sigma$	$ISMA_{2\sigma}$	$ISMA_{3\sigma}$
Round area								
≥8	52700	2143	952	32	2.25	2.18	2.1	2.04
8	36806	1535	678	26	2.26	2.18	2.1	2.03
9	10770	446	194	14	2.3	2.14	2	1.89
10	3317	126	60	8	2.1	1.85	1.66	1.5
11	1025	56	18	4	3.1	2.55	2.15	1.87
12	364	15	6	3	2.5	1.67	1.25	1
≥13	157	11	2	1	5.5	3.67	2.75	2.2
Rectangular area								
≥8	52700	2143	1880	28	1.14	1.12	1.11	1.09
8	36806	1535	1250	23	1.23	1.21	1.18	1.16
9	10770	446	365	18	1.22	1.16	1.11	1.06
10	3317	126	115	11	1.1	1	0.92	0.85
11	1025	56	34	6	1.65	1.4	1.22	1.08
12	364	15	12	3	1.25	1	0.83	0.71
≥13	157	11	5	2	2.2	1.57	1.22	1

Note: $ISMA_\sigma$, $ISMA_{2\sigma}$, and $ISMA_{3\sigma}$ denote the indices of seismicity migration activity at a level of one, two, and three standard deviations.

different geometry and shock distribution structure. This model complements the study of the migrations of earthquake sources, making it possible to determine seismicity migration criteria as an excess at a given level of significance of the mean numbers of chains created by a random spatiotemporal shock distribution. The criteria presented in the form of charts, tables, and correlation equations allow one to estimate the level of earthquake migration chains in the epicentral seismicity field of the Baikal region, areas, sections, and fault zones. In the future, this makes it possible to obtain homogeneous information for comparing the seismicity migration activity of different territories as a feature of the modern geodynamics of the lithosphere and for searching for the precursor of a strong earthquake.

In this study, we use the "index of seismicity migration activity" (ISMA) for the statistical estimation of the level of seismicity migration relative to pseudo-migrations. This ISMA is equal to the ratio of the number of earthquake

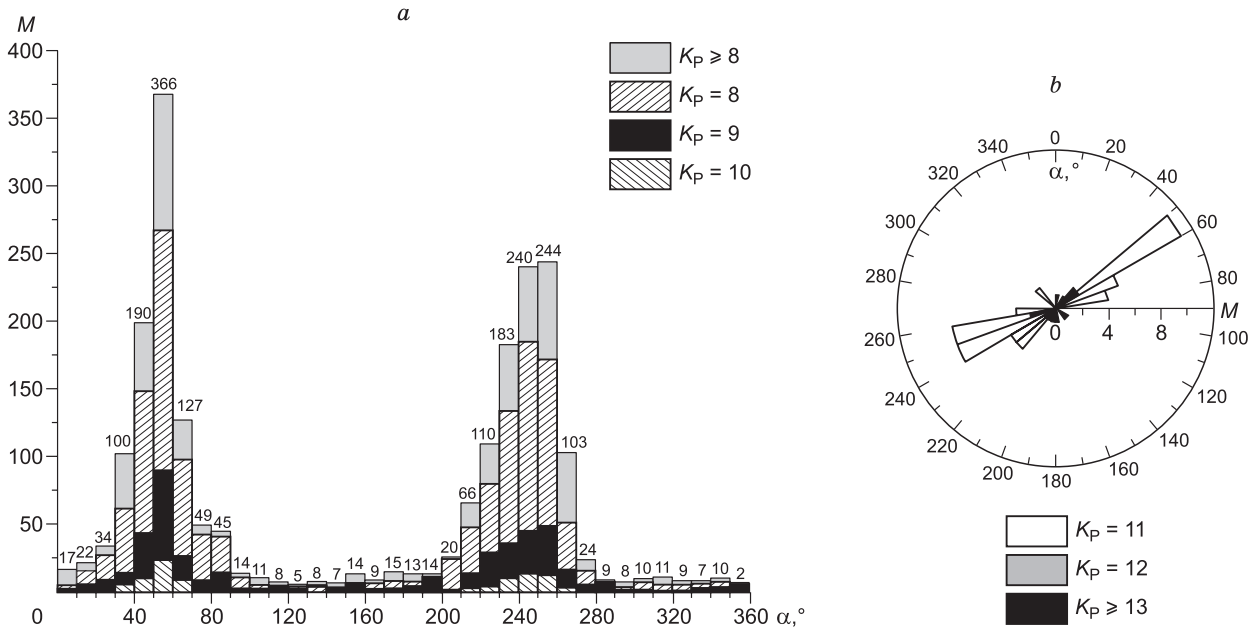

Fig. 4. Distribution histograms of the numbers of chains M with respect to azimuth α for a complete sample of data with $K_P \geq 8$ and the samples of shocks of individual classes ($K_P = 8$, $K_P = 9$, $K_P = 10$) (*a*) and the rose diagram of the numbers of chains of moderate and strong earthquakes with $K_P = 11$, $K_P = 12$, and $K_P \geq 13$ (*b*).

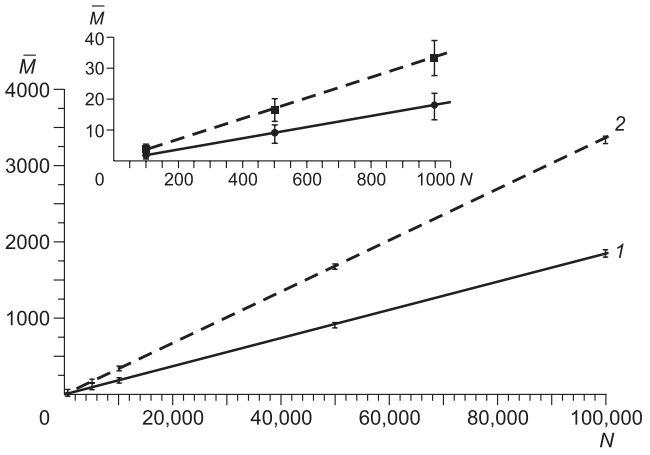

Fig. 5. Charts showing relationship $\overline{M}$ (N) for round (1) and rectangular (2) areas. The inset is made for a thousand events.

chains M, isolated among N earthquakes of the area under study, which has a round or rectangular shape and a certain size in a given sector of permissible nonlinearity q, to the average number of chains of simulation events $\overline{M}$, isolated under the same conditions in the field of random events: $ISMA = \frac{M}{\overline{M} + i\sigma}$. If ISMA > 1, then the lithosphere of the area under study contains seismicity migrations at a significance level $i\sigma$ (i = 1, 2, 3). The average number of chains of simulation events and the standard deviation σ are calculated from the data of multiple generation of artificial samples from N events distributed in the above-described manner on the surface of round or rectangular areas, and chains in each generation are distinguished in a given sector of admissible nonlinearity q. When determining the values of $\overline{M}$, multiple generations of artificial samples of size N from 10^2 to 10^5 random events are carried out so that the total number of events in the samples of each size is 10^6 events (from 10^4 to 10^5 generations, respectively). In each of these samples, the chains of events are identified and isolated, then the mean values of $\overline{M}$ and standard deviations of σ for set N are calculated, and charts for relationship $\overline{M}$ (N) are obtained for round and rectangular areas (Fig. 5). Figure 5 shows that, with an increase in the number of events N, the average number of chains $\overline{M}$ increases linearly, the spread of data is insignificant, and the charts for round and rectangular areas differ significantly.

The values of ISMA for the models of round and rectangular areas, calculated for the earthquake chains of the BRZ in different ranges of energy classes with account for 1, 2, and 3 standard deviations, are given in Table 1. As shown in Fig. 4, the distribution histograms of the numbers of chains M with respect to α have a normal form in the BRZ with maxima at azimuths of 50–60° and 240–260° for a complete sample of data and for individual classes. This type of distribution allows one to give preference to an ISMA obtained for rectangular areas. Table 1 shows that, for earthquake chains with K_P = 10 and K_P = 12 ISMA ≤ 1, i.e., seismicity migration among the shocks of such classes is minimal. In other ranges of energy classes ISMA > 1, i.e., in the BRZ lithosphere, seismicity migrations are largely present at three levels of significance. To characterize the distribution of migrating seismicity over the BRZ territory, the values of ISMA are determined in 100×100 km^2 square areas with an overlap of half the area in latitude and longitude. In Figure 6, a schematic map of the ISMA isolines in these areas is presented at a significance level of one standard deviation. It can be seen that, within the framework of the BRZ, there are several separate zones that satisfy a condition ISMA > 1. One should pay attention to the confinement of the most significant zones ISMA > 1 to rifting attractor structures (RASs) (Klyuchevskii, 2011, 2014b) and the peculiarities of their location: the zones are located to the east of RASs on the flanks and on both sides of the RASs in the central part of the BRZ. This type of ISMA distribution indicates that RASs are the sources of local deformation perturbations, which can manifest themselves as seismicity migration chains. In the extreme northeast of the BRZ, a zone of increased ISMA is observed in the vicinity of the Olyokma River, previously described as a region that forms the evolution of the Baikal Rifting to the east (Klyuchevskii and Dem'yanovich, 2006). Outside the BRZ, the high values of ISMA are observed in a zone located in the eastern part of the map, and the reason for its existence is to be clarified by detailed studies of groups of seismic events: it is possible that chains are formed in this zone during spaced industrial explosions (Klyuchevskii et al., 2015). At a significance level of two standard deviations, three zones remain on the ISMA map to the east of three RASs; at a level of three standards, only one zone is observed to the east of the North Muya RAS. The inset (Fig. 6) has charts illustrating changes in the ISMA over the years: there are four time intervals in which seismicity migrations are present at three levels of significance, and these are the maxima of 1965, 1974, 1983, and 1998. The ISMA maxima in Fig. 6 fall behind the beginning of quasi-periodic activations of RASs by three to four years, and it can be seen that the maxima of ISMA and M in Fig. 2 (1992, 1999) do not match in time.

DISCUSSION

The introduction of criteria by which seismicity migration can be described and estimated against the background of randomly distributed earthquakes does not solve the problem of isolating earthquake migration chains. Solving this problem is accompanied by difficulties caused by the large "noise" in the data on seismicity, which is due to a large number of factors contributing to the occurrence and realization of earthquakes. At present, it is impossible to determine which of the selected chains are earthquake migration chains, which is why migration perturbation parameters cannot be estimated. The low migration rates established by the predecessors from the data on strong earthquakes are

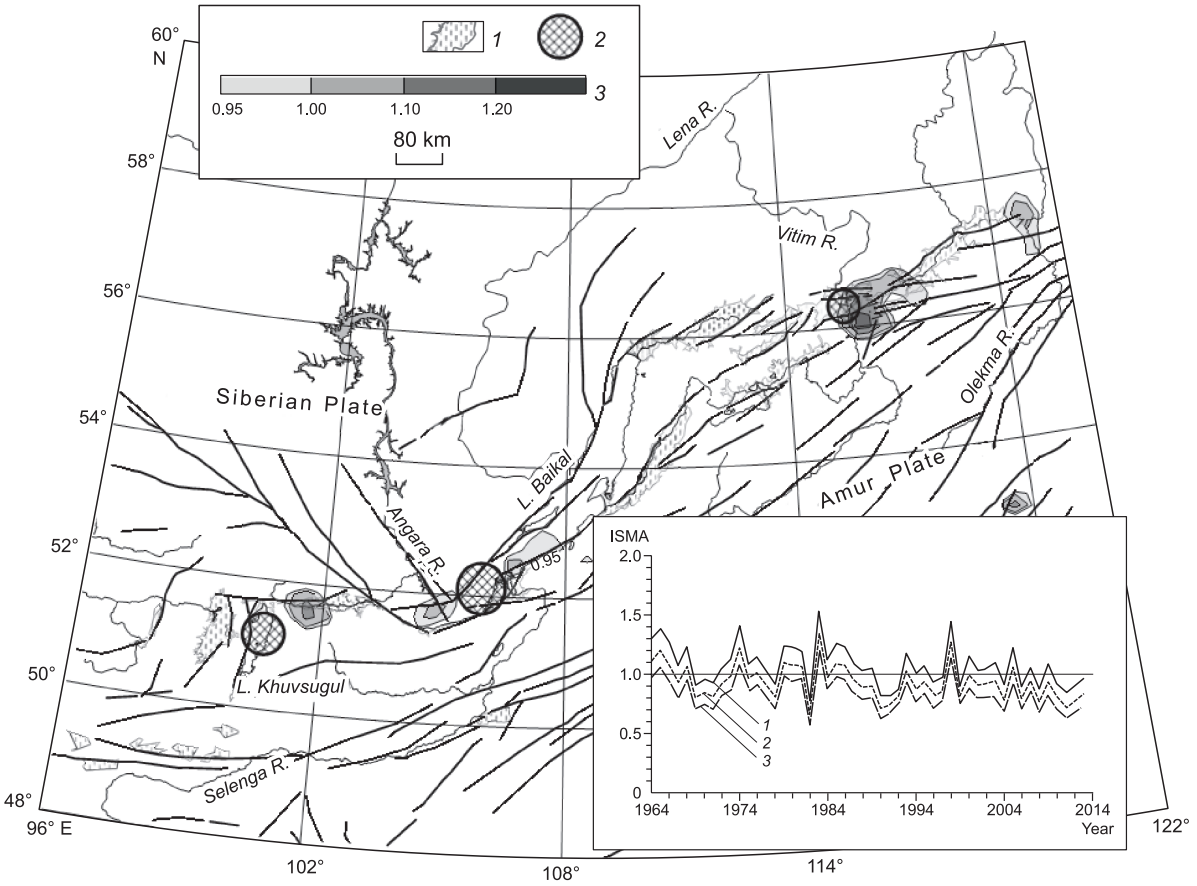

Fig. 6. Schematic map of the isolines of ISMA at a significance level of one standard deviation in areas of 100×100 km^2. Inset contains the charts (1, 2, and 3) showing the changes in ISMA over the years at a significance level of 1, 2, and 3 standard deviations, respectively. *1*, depressions, *2*, rifting attractor structures, *3*, isoline scale of the ISMA. For the rest of the legend, see Fig. 1.

due to the extremely low frequency and the approximately constant recurrent interval of such events. For weak earthquakes, everything is much more complicated: for example, in the Baikal region, from four to five thousand earthquakes with $K_P \geq 8$ are recorded annually, and, with a normal distribution, an average time between shocks is about 30 minutes. If successive shocks occur at a distance of 900 km, then the displacement velocity of "epicenters" is $v \approx 0.5$ km/s ($v \approx 1.6\times10^7$ km/year); at a distance of 90 km, the velocity is $v \approx 0.05$ km/s ($v \approx 1.6\times10^6$ km/year). It can be assumed on the basis of these estimates that, for the bulk of earthquakes in the Baikal region, the "displacement" velocities of the epicenters of successive shocks formally equal to $v \sim 10^6 \div 10^7$ km/year, and the maximum velocities are higher. Minimum velocities are set by large time intervals between strong earthquakes (tens and hundreds of years) that occurred on one fault whose length is assumed to be $l \approx 200$ km ($v \approx 200/10 \approx 20$ km/year or $v \approx 200/100 \approx 2$ km/year).

An attempt was made to solve the problem of isolating earthquake "migration" chains via the "displacement" velocities of successive epicenters in the earthquake chains of the BRZ (Klyuchevskii and Kakourova, 2018b). The goal was to find significant deviations from a normal velocity distribution due to some deterministic geophysical influencing factor that could systematically form earthquake chains and violate the distribution "normality". For that purpose, the distributions of v (velocity), l (distance), and t (time) between earthquakes were investigated for various ranges of energy classes of shocks in chains and in the samples of earthquakes that occurred in the BRZ between 1964 and 2013. New interesting results were obtained, but an attempt to separate seismicity migrations and pseudomigrations based on the "displacement" velocities of shock epicenters in the earthquake chains of the BRZ failed. Possibly, a more detailed analysis of the velocity distribution structure in the fault zones could provide information that facilitated the solution of this problem. In general, it was necessary to determine certain parameters and characteristics of geophysical and geodynamic processes that physically reflect the phenomenon of "migration" of earthquake sources. One of them could be the condition of quasi-constancy of "displacement" velocities of shock epicenters in earthquake chains, which was due to the constant propagation velocity of the influencing deformation factor.

The relationship of ISMA with the location and activations of the RASs, established in this work, define RASs as sources of deformation in the BRZ lithosphere and make it possible in the future to carry out a detailed analysis of the distribution structure of earthquake chains in the vicinity of RASs during their activation, and this can contribute to solving the problem of isolating earthquake migration chains. The eastern and northeastern location of the ISMA zones relative to the RASs indicates that the evolution of a seismic process in the form of earthquake migration chains occurs mainly in these directions, which match the orientation of the maximum horizontal compression axis in the BRZ lithosphere. A time lag of three to four years between the RAS activations and the ISMA maxima allows one to estimate the phase propagation velocity of a slow deformation perturbation of about 250–300 km/year in the first approximation, and a group velocity probably depends on the location of the territory and on the energy class value of the earthquakes used in the analysis. The phase velocity is estimated with an assumption that the perturbation covers half the BRZ (approximately 1000 km), gradually forming migration chains in this territory, and the maxima of their numbers are shown in Fig. 6 and displaced from the beginning of activation by three to four years.

Until now, there has been no specific definition of slow deformation waves, and most researchers believe that, in the loaded lithosphere, perturbations are generated, which are wavy and which affect the geomedium, geophysical fields, and processes as they propagate. The efforts of researchers are mostly focused on attempts to experimentally substantiate the existence of slow deformation waves and reveal their possible role in the migration of geodynamic processes and trigger seismic activations on the basis of methods of static processing of seismic data. Well-known theoretical attempts to explain the possible properties of slow waves in geomedia are based on the use of partial differential transfer (diffusion) equations and sine-Gordon equations. These equations are not related to deformation processes and SSS evolution, which is why they cannot clarify the physical essence of complex deformation phenomena of a loaded solid medium (Makarov et al., 2018). The modern concept of the physical nature of slow deformation waves in geomedia is formed on the basis of a synergetic approach: wavefronts in various materials and geomedia are interpreted as autowave processes caused by the instability of a loaded inhomogeneous medium, its cooperative response, and its parametric excitation (Bykov, 2005; Kuz'min, 2012). In (Zuev and Danilov, 2003; Zuev, 2006), the dynamics and physical nature of slow deformation perturbations in small samples are described using plastic metals and rock samples. It is shown that slow deformation fronts in ductile metals and rock samples are autowave too. It is assumed (Makarov and Peryshkin, 2016) that autowaves in small samples of plastic material and slow deformation autowave movements in geomedia are cooperative deformation processes similar in physical nature, which reflect the phenomenon of self-organization of the environment during deformations occurring at different scale levels. They manifest themselves as deformation fronts and/or damage fronts of different scales and propagate at low velocities in a loaded unstable medium, while the wide range of observed spatiotemporal variations in deformation autowaves is due to the multiscale fractal-block organization of solids and geomedia. It is considered that slow deformation fronts in small samples have the same physical nature as in geomedia, due to the scale invariance and self-similarity of deformation and fracture processes. One of the main results of these works is that the features of the physical state of matter and the behavior at the micro- and mesolevels manifest themselves macroscopically in nonlinear processes, and adequate mathematical models can be proposed for these processes similar in genesis.

The nonlinear wave properties of the "geophysical" lithosphere, which has a fault-block structure and complex rheology (Sadovskii et al., 1987), can be described using nonlinear differential equations, and an idea has been recently developed in mathematical models that slow deformation waves are solitons capable of the most efficient energy transfer and redistribution in a loaded elastoplastic medium. On the basis of this hypothesis, a number of authors propose to perform mathematical modeling of the fault zone dynamics and related deformation and seismic effects using both the classical sine-Gordon equation and various versions of the perturbed sine-Gordon equation (Nikolaevskii, 1995; Majewski, 2006; Vikulin et al., 2016; Bykov, 2018). Considering a loaded geomedium as a multiscale nonlinear dynamic system makes it possible to describe the observed effects of SSS evolution, including the generation of slow deformation autowaves on the mathematical basis of deformable solid mechanics (Makarov and Peryshkin, 2016). It is noted that the generation of slow deformation waves is a cooperative self-consistent deformation response to the external action of a loaded medium as a nonlinear dynamic system possessing self-organized criticality. The interactions of slow deformation fronts generated both in a plastic medium (Luders fronts) and in brittle samples demonstrate the properties of solitons – autowave fronts moving toward each other interact as elastic particles. Deformation fronts can move at a variable velocity proportional to the loading rate and stop, forming localized deformation bands. A similar behavior of wave perturbations in the form of solitons is given by solutions of the sin-Gordon equations. The very hypothesis that slow deformation fronts can possess the properties of solitons is extremely productive and can significantly advance researchers in understanding conditions for the generation of deformation waves and their possible properties. Usually, the velocity of solitons is high, reaching values orders of magnitude larger than the observed slow deformation perturbations, and, most likely, such deformation perturbations are autosolitons (Makarov et al., 2018). It can be noted that, in this study, there are some analogies with the properties of solitons: the formation and vanishing of seismicity migration chains in time, related to changes in

the SSS during activation of the RASs, and the confinement of chains to regions of maximum stress and strain (Klyuchevskii and Dem'yanovich, 2002; Klyuchevskii, 2005; Goldin et al., 2006).

Slow deformational movements are generated in the geomedium by various dynamic effects of natural and manmade origin (Psakhie et al., 2001). The studies show that the dominant force effects created by the RASs on the territory of the Mongol-Baikal Region (Klyuchevskii, 2014, 2018), are reflected through the parameters of seismicity and seismic sources in predominantly slow dynamics. The specific characteristics of impacts in the BRZ lithosphere can be determined by isolating the earthquake migration chains in the vicinity of the RASs, and this problem is solved by proceeding to a detailed analysis of the migrating seismicity in the zones of individual faults. For this purpose, it is necessary to increase the number of earthquakes used by expanding the range of weak shocks. The study should be performed separately for background and grouping seismicity (Klyuchevskii et al., 2015; 2018) as shocks in groups are essentially related events.

Transient relaxation processes in a geological-geophysical medium are reflected in the directional "displacements" of earthquake sources, and one of the main tasks of the statistical study of seismicity is to investigate these processes in manifestations of migrating seismicity. Solving this problem requires one to further develop and improve the method for identifying and isolating quasi-linear earthquake chains, which are an attribute and property of migrating seismicity. In contrast to single seismic events, which generally reflect the stochasticity of discrete seismicity, earthquake chains are an important geoinformational benchmark in the spatiotemporal distribution of earthquakes. They can be distinguished with a high degree of confidence at a given level of significance and interpreted as statistical ensembles. This other level of organization of seismicity, like strong earthquakes, characterizes the structure of the geomedium and the systemic properties of seismogenesis and modern geodynamics in generalized form. Earthquake chains, as a property of migrating seismicity, play an important role in the study of the SSS of the medium in the source zone of a strong earthquake and in fault zones and can be used for the purposes of medium- and short-term forecasting of strong earthquakes.

The methods developed, the programs implemented, and the results obtained lay the theoretical and practical basis for the technology for studying the migration of earthquake sources at various hierarchical levels of the BRZ lithosphere. The methods are developed on the basis of the available ideas about the "migrations" of earthquake sources in the fault-block lithosphere and, in general, are aimed at identifying and isolating earthquake chains in the zones of individual faults. This allows in the future to carry out a detailed formalized statistical study of the spatiotemporal and energy patterns of the migration of earthquake sources in the zones of the main seismically active faults. Of particular interest is the possibility of obtaining and analyzing data on migration chains in fault zones in order to predict strong earthquakes at the second (avalanche interaction of cracks) and third (instability) stages of avalanche-unstable cracking. The AUC model was developed in the early 1970s (Myachkin et al., 1975), and the prerequisites for its creation are the provisions of the fracture mechanics of solids and the kinetic concept of strength (Zhurkov, 1968). According to the model, a narrow region of unstable deformation is distinguished by an increased concentration of ruptures, which, in fact, represent the surface of the future main rupture (earthquake source) formed by ripping bridges between large cracks. The important thing is that such a process is self-similar at different scale levels, i.e., a large main rupture is being prepared by similar acts of the formation of smaller ruptures, possibly united by chains of migrations of weak earthquakes. A series of laboratory work carried out to simulate the process of preparing a macroscopic fracture source (Sobolev, 1993; Sobolev and Ponomarev, 2003) subjected the AUC model to a thorough check, and most of the prognostic signs were experimentally confirmed. The practical results of this work indicate the possibility of checking the formation of a strong earthquake source in the BRZ lithosphere with the implementation of chains of weak and moderate shocks in the zone of the corresponding fault.

CONCLUSION

The study is carried out using a formalized method of statistical azimuthal analysis of seismological data presented in the format of a standard catalog of earthquakes, which makes it possible to determine and allocate earthquake chains at different hierarchy levels of the lithosphere. When the method is tested, all model chains of various lengths, inserted into the initial data arrays, a significant number of earthquake chains and chains of simulated random events, are identified and isolated. The method for identifying and isolating earthquake chains is applied to the materials of the "Catalog of Earthquakes of the Baikal Region". According to the data on 52,700 earthquakes with an energy class of $K_P \geq 8$ that have occurred in the BRZ lithosphere between 1964 and 2013, a set of 2143 earthquake chains are identified and isolated with an angular sector of azimuthal analysis $q = 10°$. It is shown by analyzing the spatiotemporal and energy distribution of earthquake chains that the relationship between the numbers of isolated chains with the spatiotemporal density of shocks. The maximum number of chains is highlighted among weak shocks, and, with an increase in K_P, the number of chains decreases according to the law of recurrence of earthquakes. The azimuths of the earthquake chains correspond to the strike of the zones of the main seismogenic faults in the BRZ, and the distribution histograms of numbers of chains M with respect to azimuth α have a normal form with maxima at 50–60° and 240–260°. The migrating seismicity of the BRZ is investigated with the help

of the schematic maps of the distribution of the index of seismicity migration activity (ISMA) over the territory and the charts showing changes over the years. It is established that the local zones ISMA > 1 are manifested at three levels of significance in close proximity to the rifting attractor structures (RASs), while seismicity migration in the rest of the BRZ is not statistically obvious. The values ISMA > 1 at three levels of significance are determined three to four years after the activation of the RASs, which makes it possible to estimate the phase propagation velocity of a slow deformational perturbation of about 250–300 km/year. The results obtained indicate a direct relationship between the migrating seismicity of the BRZ with the location and activation of the RASs and allow one to conclude that the RASs are the sources of regional deformation perturbations manifested in the implementation of seismicity migration chains.

Acknowledgments: This study was partial funded by RFBR (project 14-05-00308_a, project 17-57-44006), RFBR and MECSS, project number 20-55-44011.

REFERENCES

Bot, M., 1968. Prediction of Earthquakes [in Russian]. Mir, Moscow.

Box, G.E.P., Muller, M.E.A., 1958. Note on the generation of random normal deviates. Ann. Math. Stat. 29 (2), 610–611.

Bykov, V.G., 2005. Strain waves in the Earth: theory, field data, and models. Russian Geology and Geophysics (Geologiya i Geofizika) 46 (11), 1158–1170 (1176–1190).

Bykov, V.G., 2018. Prediction and observation of deformation waves of the Earth. Geodinamika i Tektonofizika 9 (3), 721–754.

Dem'yanovich, V.M., Dem'yanovich, M.G., Klyuchevskii, A.V., 2007. Main faults of the Baikal Rift Zone and the seismicity formed by them, in: Problems of Modern Seismology and Geodynamics of the Central and Eastern Asia [in Russian]. Irkutsk.

Dem'yanovich, V.M., Klyuchevskii, A.V., 2018a. Faults and source parameters of earthquakes in the Baikal Rift Zone: dip angles of fault planes. Dokl. Earth Sci. 479 (5), 433–438.

Dem'yanovich, V.M., Klyuchevskii, A.V., 2018b. Seismicity model and its characteristics in an additive fault zone, in: Solar-Terrestrial Relations and Geodynamics of the Baikal-Mongolia Region: The Results of Many Years of Research and the Scientific-Educational Policy (for the 100th Anniversary of the Irkutsk State University) [in Russian]. Izd. Irk. Gos. Univ., Irkutsk.

Golenetsky, S.I., 1990. Problems of seismicity of the Baikal rift zone. J. Geodyn. 11, 293–307.

Guberman, Sh.A., 1979. D-Waves and earthquakes. Theory and analysis of seismic observations. Vychislitel'naya Seismologiya, No. 12, 158–188.

Kakourova, A.A., Klyuchevskii, A.V., 2017. Simulation base model of migration seismicity: fault zone. Vestnik Irkutskogo Gosudarstvennogo Tekhnicheskogo Universiteta, Vol. 21, 6 (125), 49–59, doi: 10.21285/1814-3520-2017-6-49-59.

Kakourova, A.A., Klyuchevskii, A.V., 2018. BRZ Earthquake Chains Database. Registration number: 2018621789. Registration date: November 14, 2018.

Kasahara, K., 1981. Earthquake Mechanics. Cambridge University Press.

Klyuchevskii, A.V., 2005. Modern geodynamic processes in the lithosphere of the Baikal Rift Zone. Geotectonics 39 (3), 186–199.

Klyuchevskii, A.V., 2007. Stresses and seismicity at the present stage of evolution of the Baikal rift zone lithosphere. Izv. Phys. Solid Earth 43 (12), 992–1004, doi: 10.1134/S1069351307120026.

Klyuchevskii, A.V., 2011. Attractor structure of riftogenesis in the lithosphere of Baikal Rift System. Dokl. Earth Sci. 437 (1), 407–411, doi: 10.1134/S1028334X11030135.

Klyuchevskii, A.V., 2014a. Focal parameters of strong earthquakes of Baikal Area: Ehe main regularities. Dokl. Earth Sci. 457 (2), 971–975, doi: 10.1134/S1028334X14080054.

Klyuchevskii, A.V., 2014b. Rifting attractor structures in the Baikal Rift System: Location and Effects. J. Asian Earth Sci. 88, 246–256, doi: 10.1016/j.jseaes.2014.03.009.

Klyuchevskii, A.V., 2018. Seismic geodynamics of the Mongolian lithosphere. Fizicheskaya Mezomekhanika, No. 21 (2), 118–131.

Klyuchevskii, A.V., Dem'yanovich, V.M., 2002. Seismic strain state of the Earth's crust in the Baikal Region. Dokl. Earth Sci. 383 (2), 178–182.

Klyuchevskii, A.V., Dem'yanovich, V.M., 2006. Stress-strain state of the lithosphere in the southern Baikal region and northern Mongolia from data on seismic moments of earthquakes. Izv. Phys. Solid Earth 42 (5), 416–428.

Klyuchevskii, A.V., Zuev, F.L., 2007. Structure of the epicenter field of earthquakes in the Baikal region. Dokl. Earth Sci. 415 (2), 944–949.

Klyuchevskii, A.V., Kakourova, A.A., 2016. Base simulation model of migrating seismicity. Vestnik Irkutskogo Gosudarstvennogo Tekhnicheskogo Universiteta, No. 8 (115), 74–84.

Klyuchevskii, A.V., Kakourova, A.A., 2018a. The main criteria for allocating earthquake chains in the Baikal Region lithosphere. Izvestiya Irkutskogo Gosudarstvennogo Universiteta Ser. Nauki O Zemle, No. 23, 64–73.

Klyuchevskii, A.V., Kakourova, A.A., 2018b. Displacement velocity of epicenters in the earthquake chains of the Baikal Region, in: Geodynamic Evolution of the Lithosphere of the Central Asian Mobile Belt (from Ocean to Continent) [in Russian]. IZK SO RAN, Irkutsk.

Klyuchevskii, A.V., Dem'yanovich, V.M., Klyuchevskaya, A.A., Zuev, F.L., Kakourova, A.A., Chernykh, E.N., Bryzhak, E.V., 2015. Grouping Seismicity of the Baikal Region (Relevant Problems in the Science of the Baikal Region) (in Russian). Izd. Instituta Geografii SO RAN, Irkutsk.

Klyuchevskii, A.V., Kakourova, A.A., Klyuchevskaya, A.A., Dem'yanovich, V.M., Chernykh, E.N., 2018b. Patent No. 2659334. Method for determining earthquake chains in an epicentral seismicity field. Registered in the State Register of Inventions of the Russian Federation on July 29, 2018. Bulletin No. 19.

Kuz'min, Yu.O., 2012. Deformation autowaves in fault zones. Izv. Phys. Solid Earth 48 (1), 1–16.

Levina, E.A., Ruzhich, V.V., 2015. Seismicity activity migrations studied using space-time diagrams. Geodinamika i Tektonofizika, No. 6 (2), 225–240.

Lobatskaya, R.M., 1987. Structural Zonality of Faults [in Russian]. Nedra, Moscow.

Logachev, N.A., 2003. History and geodynamics of the Baikal rift. Geologiya i Geofizika (Russian Geology and Geophysics) 44 (5), 391–406 (373–387).

Lukk, A.A., 1978. Spatiotemporal sequences of weak earthquakes in the Garm Region. Fizika Zemli, No. 2, 25–37.

Majewski, E., 2006. Rotational energy and angular momentum of earthquakes, in: Teisseyre, R., Majewski, E., Takeo (Eds.), Earthquake Source Asymmetry, Structural Media and Rotation Effects. Springer, Berlin, Heidelberg, https://doi.org/10.1007/3-540-31337-0_16.

Makarov, P.V., Khon, Yu.A., Peryshkin, A.Yu., 2018. Slow deformation fronts. Model and features of distribution. Geodinamika i Tektonofizika 9 (3), 755–769.

Makarov, P.V., Peryshkin, A.Yu., 2015. Modeling "slow movements" – Auto waves of non-elastic deformation in ductile and brittle materials and media. AIP Conf. Proc. 1683, Article 020136.

Malamud, A.S., Nikolaevsky, V.N., 1983. Periodicity of the Pamir – Hindu Kush earthquakes and tectonic waves in subducted lithospheric plates. Dokl. Akad. Nauk SSSR 269 (6), 1075–1078.

Misharina, L.A., Solonenko, A.V., 1990. Influence of the block divisibility of the Earth's crust on seismicity distribution in the Baikal Rift Zone, in: Seismicity of the Baikal Rift. Prognostic Aspects [in Russian]. Nauka, Novosibirsk.

Mogi, K., 1968. Migration of seismic activity. Bull. Earthquake Res. Inst. 46, 53–74.

Myachkin, V.I., Kostrov, B.V., Sobolev, G.A. Shamina, O.G., 1975. Fundamentals of source physics and earthquake precursors, in: Physics of the Earthquake Source [in Russian]. Nauka, Moscow.

Nevskii, M.V., Artamonov, A.M., Riznichenko, O.Yu., 1991. Deformation waves and seismicity energetic. Dokl. Akad. Nauk SSSR 318 (2), 316–320.

Nikolaevskii, V.N., 1995. Mathematical modeling of solitary deformation and seismic waves. Dokl. Akad. Nauk 341 (3), 403–405.

Novopashina, A.V., 2013. Methods for detecting seismic activity migrations in the Baikal Region by means of GIS. Geoinformatika, No. 1, 33–36.

Psakh'e, S.G., Ruzhich, V.V., Smekalin, O.P., Shilko, E.V., 2001. Geological media responses under dynamic influences. Fizicheckaya Mezomekhanika, No. 4 (1), 67–71.

Richter, C.F., 1958. Elementary Seismology. W.H. Freeman and Co, San Francisco.

Sadovskii, M.A., Bolkhovitinov, L.G., Pisarenko, V.F., 1987. Deformation of the Geophysical Medium and the Seismic Process [in Russian]. Nauka, Moscow.

Sherman, S.I., 2013. Deformation waves as a trigger mechanism of seismic activity in the seismic zones of the continental lithosphere. Geodinamika i Tektonofizika, No. 4 (2), 83–117.

Sherman, S.I., Gorbunova, E.A., 2008. Wave nature of fault activation in Central Asia based on seismic monitoring. Fizicheskaya Mezomekhanika, No. 11 (1), 115–122.

Sobolev, G.A., 1993. Basics of Earthquake Prediction [in Russian]. Nauka, Moscow.

Sobolev, G.A., Ponomarev, A.V., 2003. Earthquake Physics and Precursors [in Russian]. Nauka, Moscow.

Ulomov, V.I., 1993. Seismogeodynamic activation waves and long-term forecast of earthquakes. Fizika Zemli, No. 4, 43–53.

Vikulin, A.V, Dolgaya, A.A., Gerus, A.I., 2016. Wave Geodynamic Process Within the Framework of the Block Geomedium of the Crust, in: Proc. Fourth Tectonophysics Conf. "Tectonophysics and Relevant Questions of Sciences about the Earth". Vol. 1. Schmidt Institute of Physics of the Earth RAS, Moscow.

Vikulin, A.V., 2003. Physics of the Wave Seismic Process [in Russian]. Kamch. Gos. Pedagog. Univer., Petropavlovsk-Kamchatsky.

Vil'kovich, E.V., Guberman, Sh.A., Keilis-Borok, V.I., 1974. Tectonic deformation waves at large faults. Dokl. Akad. Nauk SSSR 219 (1), 77–80.

Zhurkov, S.N., 1968. Kinetic conception of strength of solids. Vestnik Akad. Nauk SSSR, No. 3, 46–52.

Zuev, L.B., 2006. Wave nature of plastic flow. Macroscopic autowaves of deformation localization. Fizicheskaya Mezomekhanika, No. 9 (3), 47–54.

Zuev, L.B., Danilov, V.I., 2003. Slow autowave processes in deformation of solids. Fizicheskaya Mezomekhanika, No. 6 (1), 75–94.

http://www.seis-bykl.ru/ Baikal Branch of the Federal Research Center "Unified Geophysical Service of the Russian Academy of Sciences".

Editorian responsibility: V.S. Selesnev